Journal of Alloys and Compounds 480 (2009) L9–L12

Contents lists available at ScienceDirect

Journal of Alloys and Compounds

journal homepage: www.elsevier.com/locate/jallcom

Letter

Catalyst-free shape controlled synthesis of In_2O_3 pyramids and octahedron: Structural properties and growth mechanism

Ahsanulhaq Qurashi[a], E.M. El-Maghraby[b], Toshinari Yamazaki[a,*], Toshio Kikuta[a]

[a] Department of Engineering, Toyama University, 3190 Gofuku, Toyama 930-8555, Japan
[b] Department of Physics, Assiut University, Assiut 71516, Egypt

ARTICLE INFO

Article history:
Received 20 December 2008
Received in revised form 19 January 2009
Accepted 22 January 2009
Available online 6 February 2009

Keywords:
In_2O_3
Pyramids
Octahedrons
FESEM
TEM

ABSTRACT

In_2O_3 pyramids and octahedrons were synthesized on a silicon substrate by catalyst-free and improved chemical vapor deposition in order to reduce the influence of undesired doping or impurities on the observed properties, directly from metallic indium by controlled oxidation. These single crystalline In_2O_3 structures have potential use in ultra-sensitive gas and chemical sensors.

1. Introduction

Metal oxides semiconductors have stimulated great interest and extensive research due to their novel electronic and optical properties [1–5]. Among them, indium oxide (In_2O_3), is an exceedingly important wide bandgap (3.6 eV) oxide material and has been widely used for ultra-sensitive toxic gas detectors, chemical sensors and optoelectronic devices [6–9]. There have been an increasing number of reports on the synthesis of In_2O_3 structures by using various methods such as carbothermal reduction, thermal evaporation, chemical vapor deposition, laser ablation, etc. [10–13]. In spite of favoring high-quality In_2O_3 structures these techniques remain constrained by the use of catalyst, high reaction temperature and high vacuum system. Wei et al. reported the growth of In_2O_3 octahedrons on indium tin oxide (ITO) substrate at low temperature [14]. They used ITO as seed layer to precipitate In_2O_3 octahedrons. Kumar et al. also reported the synthesis of In_2O_3 octahedrons using active carbon at higher temperature and at longer reaction time of 12 h [11]. However, controlled-synthesis of the In_2O_3 at low temperature is still a challenging task. The present letter reports on catalyst-free, low temperature and controlled growth of In_2O_3 pyramids and octahedrons by improved chemical vapor deposition. The shape of In_2O_3 structures was modulated by regulating the reaction temperature.

2. Experimental details

The synthesis of In_2O_3 structures was performed in an improved chemical vapor deposition system. The schematic diagram for chemical vapor deposition is shown in Fig. 1. The one end of quartz tube made the airflow reverse and increased the saturation ratio of the reagent species and the other end was kept open with small outlet, and the location of the source under the substrate, which was placed properly and not down stream like conventional CVD systems. In a typical experimental procedure 0.5 g of high-purity indium grains was put under a silicon wafer placed in an alumina boat. Before heating, the tube chamber was purged for 30 min with 100 mL/min^{-1} high purity Ar, and then the furnace was heated to 800 °C at a rate of 25 °C/min and kept at this temperature for 60 min. After the reaction, a layer of yellow product was found deposited on the silicon wafer. In order to study extensively the effect of reaction temperature on the morphology and shape of In_2O_3 structures, the synthesis was also carried out at 700 and 900 °C. The crystalline phase and morphological and structural features of the products were investigated by X-ray diffraction (XRD) (Shimadzu XRD 6100 Cu Kα (0.15419 nm) radiation), field emission scanning electronic microscope (FESEM), and high-resolution transmission electron microscopy (TEM TOPCON EM-002B).

3. Results and discussion

Fig. 2 shows XRD pattern of In_2O_3 structures grown at 800 °C. All the peaks are indexed to the pure cubic phase with lattice parameter a = 1.011 Å (JCPDS No. 89–4595), indicating that pure phase of In_2O_3 is obtained under prevailing conditions. However, no impurities existed in the sample under the prevailing reaction conditions.

Fig. 3 shows the FESEM images of the In_2O_3 crystals formed at 700 °C, pyramids formed at 800 °C and octahedrons formed at 900 °C. Fig. 3(a and b) shows high density In_2O_3 triangular shaped In_2O_3 crystals. Fig. 3(c) reveals that the product consists

* Corresponding author. Fax: +81 76 445 6882.
E-mail address: yamazaki@eng.u-toyama.ac.jp (T. Yamazaki).

0925-8388/$ – see front matter © 2009 Elsevier B.V. All rights reserved.
doi:10.1016/j.jallcom.2009.01.112

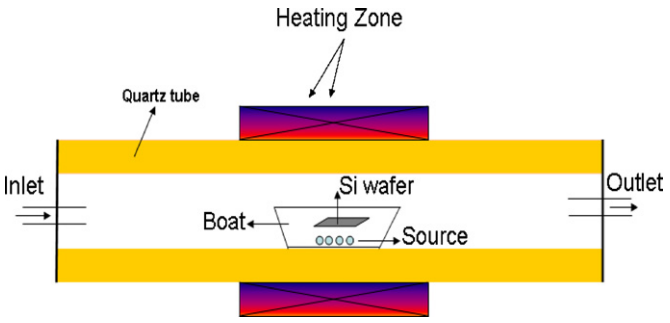

Fig. 1. Schematic diagram of chemical vapor deposition system.

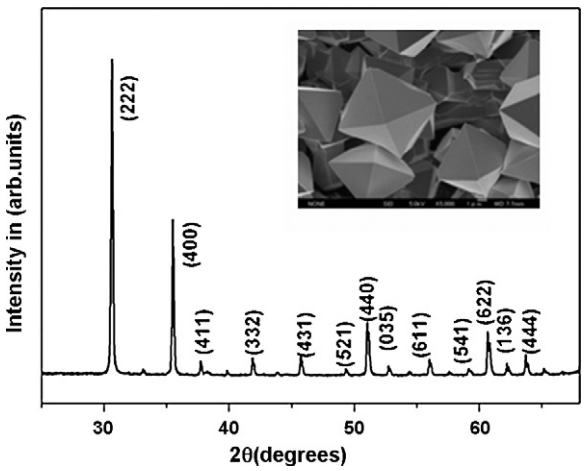

Fig. 2. XRD spectra of In_2O_3 pyramids.

of high-density pyramids grown on the entire surface of the substrate at 800 °C. Fig. 3(d) shows high magnification FESEM image of single pyramids. The pyramids have four equilateral triangles and a square. In Fig. 3(e) one can observe high-density octahedrons at 900 °C. Fig. 3(e) shows high magnification FESEM image of an octahedron. A regular In_2O_3 octahedron is composed of eight well-faceted equilateral triangles, four of which meet at each nanovertex. Each side of triangle has length ~1.5 μm. All the surfaces of pyramids and octahedrons are smooth and there are no obvious structural defects.

Further structural characterization of In_2O_3 structures was performed by TEM analysis. For the TEM analysis, the as-grown pyramids and octahedrons were ultrasonically dispersed from the substrate into acetone. A drop of suspension was placed on a TEM grid. Fig. 4(a and b) shows the TEM images of single In_2O_3 pyramid and octahedron, respectively. The SAED pattern in Fig. 4(a) shows single crystalline In_2O_3 with cubic structure and indicates that pyramids grow along [0 0 1] direction. The lattice spacing of (2 0 0) is equal to 0.50 nm due to In_2O_3 structure for pyramids oriented along [0 0 1] direction. The EDX spectrum (Fig. 4(d)) shows the appearance of In and O peaks from pyramids, thus confirming that faceted single crystalline pyramids and octahedrons do not include impurities.

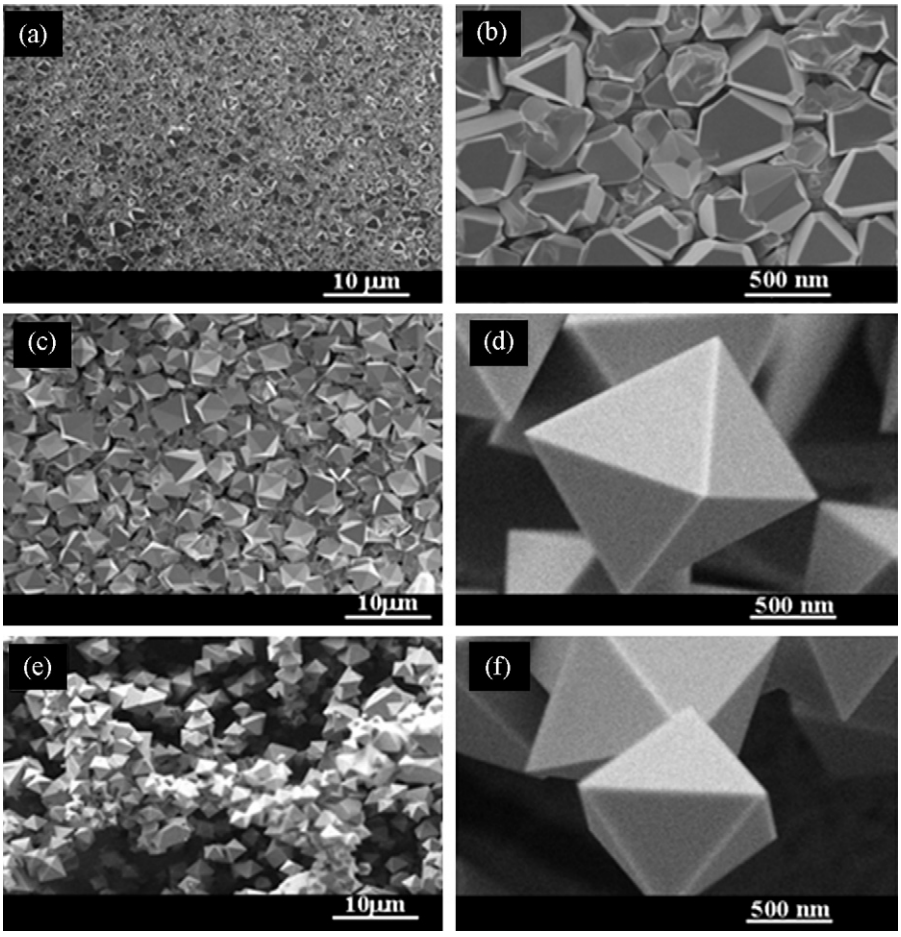

Fig. 3. Low and high magnification FESEM images of In_2O_3 crystals (a and b) pyramids (c and d) and octahedrons (e and f).

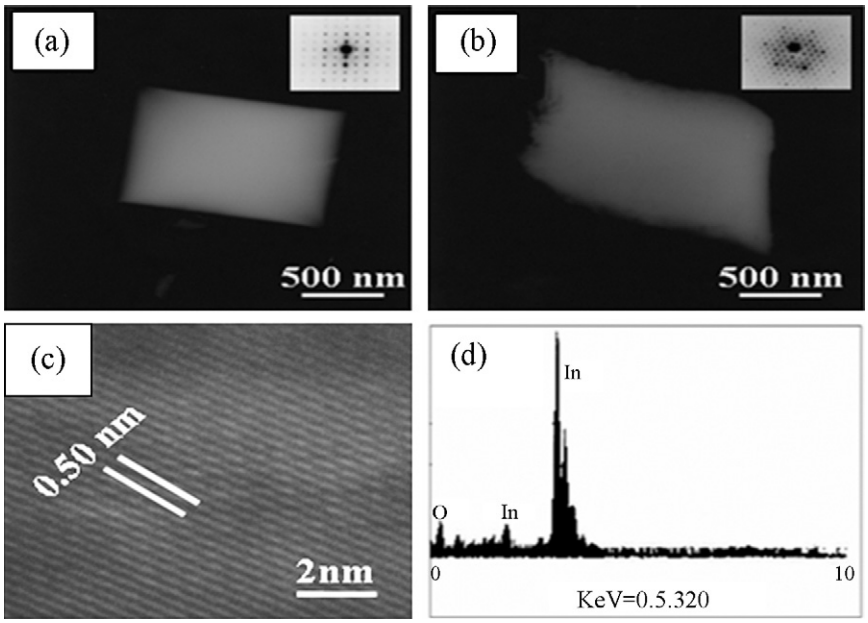

Fig. 4. (a and b) Are high magnification TEM images of pyramids and octahedrons respectively. The insets of (a and b) show SAED patterns. (c) is a HRTEM image for pyramids. (d) shows an EDX spectrum for pyramids.

3.1. Growth mechanism of In_2O_3 pyramid and octahedron structures

In the absence of the catalyst, In_2O_3 pyramids and octahedrons were growing via a vapor–solid (VS) mechanism. A schematic illustration for the formation of In_2O_3 pyramids and octahedrons is shown in Fig. 5. Initially the melting of indium starts at 156.6 °C, and then the indium vapor combine with the residual oxygen to form oxidized In cluster Fig. 5(b). The saturated vapor pressure of In is much higher than that of In_2O_3 at the same temperature. As a result, such circumstances lead to a higher super saturation ratio of oxidized In vapor in the surrounding area of central heating region. When the reaction temperature further increases, these oxidized In clusters act as the nucleation centre for the anisotropic growth of In_2O_3 nuclei Fig. 5(c). In principle, crystal growth and morphology are directed by extrinsic and intrinsic factors. We presume that the saturated vapor pressure of liquid state In metal increased remarkably, whereas the saturated vapor pressure of solid-state In_2O_3 increased unobtrusively during the elevated reaction temperatures. Consequently, the supersaturation ratio of the oxidized In vapor increased conspicuously. The growth of these In_2O_3 nuclei leads to the formation of anisotropic In_2O_3 structures with increasing elapsed time and increasing temperature. We obtained distinct morphologies of triangular crystals, pyramids and octahedrons under distinct reaction conditions. In_2O_3 triangular crystals were formed at low temperature of 700 °C while as pyramids and octahedrons obtained at 800 and 900 °C. The faces contain the crystals habit corresponds directly with most energetically

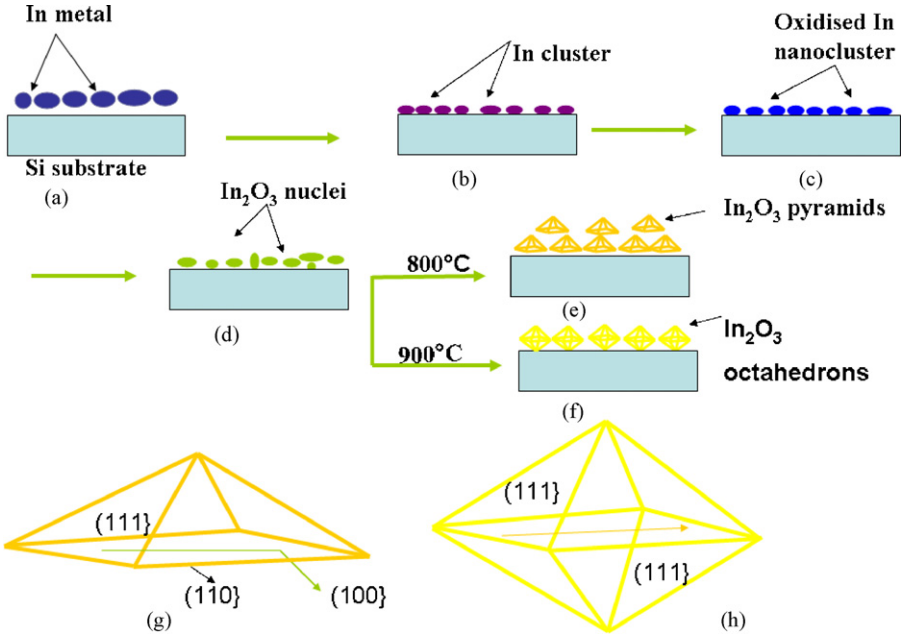

Fig. 5. Schematic illustration of growth mechanism of In_2O_3 pyramids and octahedrons.

promised stable atomic planes in the lattice. These planes have low miller indices ($h\,k\,l$). Low index faces are normally stable because they contain tightly packed arrays of sturdily bonded atoms. The magnitude relation between the surface energies of low index crystallographic planes of In_2O_3 with a bcc structure is expressed by $\gamma\{1\,1\,1\} < \gamma\{1\,0\,0\} < \gamma\{1\,1\,0\}$ [15]. The anisotropic crystal growth rate (r) perpendicular to a plane is proportional to their surface energies. The evolution of triangular shaped In_2O_3 crystals occurs at low temperature (700 °C) due to an increase in the area of $\{1\,1\,1\}$ relative to $\{1\,0\,0\}$ plane. The pyramid shape is consistent with the cubic crystal structure of In_2O_3. In the In_2O_3 cubic structure, the $\{0\,0\,1\}$ family planes contain the three equivalent planes $(1\,0\,0)$, $(0\,1\,0)$, and $(0\,0\,1)$, which are perpendicular to the three directions $[1\,0\,0]$, $[0\,1\,0]$, and $[0\,0\,1]$ respectively. Pyramids bounded by $\{1\,1\,1\}$ facets with the highest $(1\,1\,1)$ to that of $(1\,0\,0)$ surface energy ratio possess the lowest surface energy [16]. The difference of surface energies among $\{1\,1\,0\}$, $\{1\,0\,0\}$, $\{1\,1\,1\}$ facets can lead to their different growth rates [17–19]. Thus, the high supersaturation ratio due to higher temperature (900 °C) makes the substantial effect of the surface energy difference on the growth and morphology. As a result, the crystal growth rates perpendicular to $\{1\,1\,1\}$, $\{1\,0\,0\}$, and $\{1\,1\,0\}$ facets become quite close, and growth of octahedrons crystals can be realized. It is assumed that due to higher temperature the species absorbed on the side surface had high surface energy. The results mentioned above demonstrated that elevated reaction temperature favored high growth rate and appearance of low surface energy $\{1\,1\,1\}$ planes. This behavior was further clarified by the fact that amorphous shape In_2O_3 crystals were obtained at a temperature of 700 °C. Thus the low surface energy planes at higher temperature guided the formation of well-faceted highly crystalline and anisotropic pyramids and octahedrons respectively.

In conclusion, catalyst-free synthesis of pyramids and octahedrons were carried out on silicon substrate. Structural analysis reveals that In_2O_3 structures are single crystalline with cubic structure. We believe that these In_2O_3 structures with special morphology can be potentially useful in fabricating high sensitivity gas sensors, where well-defined crystal surface is essential.

Acknowledgement

Ahsanulhaq Qurashi is thankful to venture business laboratory of Toyama University for post-doctoral fellowship.

References

[1] N.K. Reddy, Q. Ahsanulhaq, J.H. Kim, M. Devika, Y.B. Hahn, Nanotechnology 18 (2007) 445710.
[2] Q. Ahsanulhaq, J.H. Kim, Y.B. Hahn, Nanotechnology 18 (2007) 485307.
[3] Q. Ahsanulhaq, A. Umar, Y.B. Hahn, Nanotechnology 18 (2007) 115603.
[4] Q. Ahsanulhaq, S.H. Kim, J.H. Kim, Y.B. Hahn, Mater. Res. Bull. 43 (2008) 3483.
[5] Q. Ahsanulhaq, J.H. Kim, N.K. Reddy, Y.B. Hahn, J. Indus. Eng. Chem. 14 (2008) 578.
[6] H.D. Zhang, C. Li, L.X. Liu, S. Han, T. Tang, W.C. Zhou, Appl. Phys. Lett. 83 (2003) 1845–1847.
[7] K. Soulantica, L. Erades, M. Sauvan, F. Senocq, A. Maisonnat, B. Chaudret, Adv. Funct. Mater. 13 (2003) 553–561.
[8] C. Li, D.H. Zhang, L.X. Liu, S. Han, T. Tang, J. Han, W.C. Zhou, Appl. Phys. Lett. 82 (2003) 1613–1615.
[9] P. Nguyen, T.H. Ng, T. Yamada, M.K. Smith, J. Li, J. Han, M. Meyyappan, Nano Lett. 4 (2004) 651–657.
[10] Q. Wan, M. Wei, D. Zhi, J.L. MacManus-Driscoll, M.G. Blamire, Adv. Mater. 18 (2006) 234–238.
[11] M. Kumar, V. Singh, F. Singh, K.V. Lakshmi, B.R. Mehta, J.P. Singh, Appl. Phys. Lett. 92 (2008) 171907–171909.
[12] H.W. Kim, N.H. Kim, C. Lee, Appl. Phys. A 81 (2005) 1135–1138.
[13] C. Li, D. Zhang, S. Han, X. Liu, T. Tang, C. Zhou, Adv. Mater. 15 (2003) 143–146.
[14] M. Wei, D. Zhi, J. Driscoll, Nanotechnology 17 (2006) 3523.
[15] Y.G. Yan, Y. Zhang, H.B. Zeng, L.D. Zhang, Cryst. Growth Des. 5 (2007) 940–943.
[16] Z.L. Wang, J. Phys. Chem. B 104 (2000) 1153–1175.
[17] Q. Tang, W. Zhou, W. Zhang, S. Ou, K. Jiang, W. Yu, Y.T. Qian, Cryst. Growth Des. 5 (2005) 147–150.
[18] Y. Zhang, H. Jia, D. Yu, X. Luo, Z. Zhang, X. Chen, J. Mater. Res. 18 (2003) 2793–2798.
[19] M. Zhong, M. Zheng, L. Ma, Y. Li, Nanotechnology 18 (2007) 465605.